

Momentum-dependent dielectric function of polyacetylene

John J. Ritsko

Xerox Webster Research Center, Webster, New York 14580

(Received 16 February 1982)

The momentum-dependent dielectric function of *trans*-polyacetylene was computed from electron-energy-loss spectra for momenta q between 0.1 and 0.7 \AA^{-1} . The spectrum of direct interband transitions broadens and shifts to higher energy with increasing q . The observed linear plasmon dispersion is well correlated with interband excitation spectra calculated in a simple tight-binding band-structure model. The fundamental absorption threshold is dominated by excitonic effects leading to a weakly dispersive absorption edge.

Conjugated polymer molecules are interesting systems in which to study the electronic structures and electronic excitations of quasi-one-dimensional semiconductors. These systems are characterized by wide energy bands with a small gap separating valence and conduction bands. In conjugated polymers the bands of interest are made up of the carbon $2p$ orbitals sticking out of the plane of the molecule, the π orbitals. The simplest examples of such materials are polyacetylene with alternating single and double bonds, and polydiacetylene with alternating single, double, and triple bonds. The π bands of these polymers are quite similar and their electronic structure has been calculated by many methods.¹⁻⁶ The nature of the electronic structure in these materials is thus an active area of current theoretical and experimental research. Much attention has focused on the fundamental absorption edge. The relative contributions of direct interband transitions,³ indirect transitions,^{7,8} excitonic,^{5,6} local-field,⁹ and correlation effects⁴ at this threshold are controversial. In addition, excitations above the band gap in polyacetylene give rise to a collective mode, a plasmon, which exhibits an unusual linear dispersion relation.⁸ To further the understanding of electronic excitations in conjugated polymers, we have carried out a series of measurements of the momentum dependence of electron-energy-loss spectra in well-characterized thin films of *trans*-polyacetylene. From these data we compute the momentum-dependent dielectric function $\epsilon(q, E)$ and compare the experimental results with simple calculations of interband transitions between one-dimensional tight-binding energy bands. The plasmon dispersion is shown to correlate reasonably well with the momentum dependence of interband transitions and the possible na-

ture of excitonic effects at the fundamental absorption edge is described.

The samples used in the present study were prepared at the University of Pennsylvania by the chemistry group headed by A.G. MacDiarmid. Polyacetylene was made as a very thin film supported on a platinum screen. The screen was cut to the size necessary for use in the electron-energy-loss spectrometer. The sample was converted to 100% *trans*-isomer by heating in vacuum at 160°C for 20 min. The original films were purple in transmission, indicating a mixture of *cis*- and *trans*-isomers. After the heat treatment they were a royal blue indicative of *trans*-polyacetylene. During all preparation and measurement procedures the samples were never exposed to ambient conditions. They were handled in pure argon at atmospheric pressure or vacuum. Electron microscopy showed the samples to be fibrous and highly crystalline with randomly oriented crystallites.

Energy-loss spectra were obtained for 80-keV electrons with an energy resolution of 0.1 eV and a momentum resolution of 0.05 \AA^{-1} . Energy-loss spectra from 0 to 10 eV, as a function of momentum, are given in Fig. 1(a), and a typical spectrum from 0 to 100 eV at $q=0.1 \text{\AA}^{-1}$ is shown in Fig. 1(b). These spectra are very similar to those reported previously.⁸ The earlier data were obtained on samples prepared by a different method. The samples had not been completely isomerized. Moreover, the earlier samples had been exposed to ambient conditions for a short period of time (0.5 h). The fact that the present measurements agree with the previous study⁸ indicates the relative insensitivity of electronic excitations in polyacetylene to the difference in *cis-trans* content or a small amount of oxygen. The spectrum in Fig.

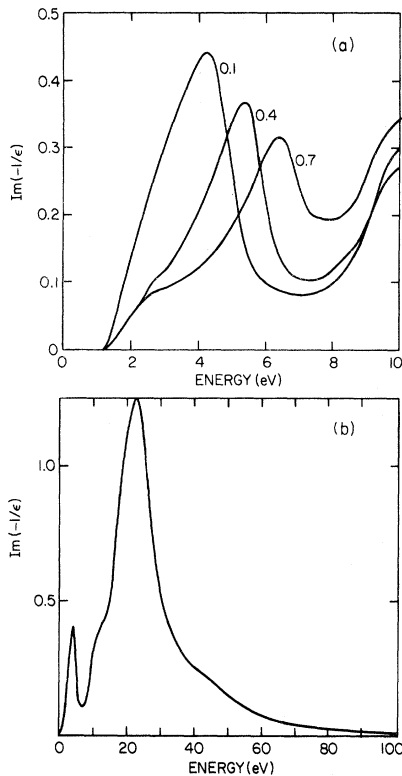


FIG. 1. (a) Momentum dependence of energy-loss spectra in polyacetylene for q in \AA^{-1} . (b) Uncorrected energy-loss spectrum at $q = 0.1 \text{\AA}^{-1}$ from 0 to 100 eV.

1(b) shows that the effective film thickness was $< 500 \text{\AA}$, since the double-scattering probability of the strongest peak in the spectrum, a plasmon at 22.5 eV, is nearly negligible. The relative weakness of multiple inelastic scattering events in the energy-loss spectra meant that large corrections for these effects were not necessary and that the calculation of the momentum-dependent dielectric function was greatly simplified.

The principal stumbling block to obtaining information about the momentum-dependent dielectric function of polyacetylene is that the samples contain randomly oriented crystallites each of which is highly anisotropic.⁷ Therefore, the measured energy-loss probability at a particular momentum transfer consists of an average over all possible directions of the momentum q of all excitations with that particular value of q . Thus, the result of our calculation will be an averaged response function in that sense. In the limit of small q the dielectric response function measured in an energy-loss experiment becomes equivalent to the optical dielectric function, and the degree of anisotropy, measured optically, should also be

present in the energy-loss spectra. In the region from 0 to 4 eV, optical absorption occurs only for excitations polarized along the polymer chain,⁷ and so the energy-loss spectrum at $q = 0.1 \text{\AA}^{-1}$ (the smallest momentum transfer we can accurately measure) most likely contains only excitations polarized in that direction.⁸ Therefore, in our earlier Kramers-Kronig analysis of $q = 0.1 \text{\AA}^{-1}$ energy-loss data, the spectra were normalized so as to reproduce the value of the real part of the dielectric function parallel to the chains at low energy, namely $\epsilon_1 = 10$ (Refs. 8 and 10).

Here we wish to extend our analysis to larger values of the momentum transfer where we can no longer use the $q = 0$ dielectric constant to normalize the data. Following Bringans and Liang,¹¹ the energy-loss spectra at finite q were normalized so as to reproduce values of $\epsilon_1(q, 0)$ calculated using the Thomas-Fermi theory of Resta.¹² This theory treats an isotropic semiconductor with an equivalent valence Fermi momentum k_F , where $k_F = (3\pi n_0)^{1/3}$ and n_0 is the valence electron density. If $p^2 = 4k_F/\pi$, then, with the use of atomic units,

$$\epsilon_1(q, 0) = (p^2 + q^2) / \left[\frac{p^2}{\epsilon_1(0, 0)} \frac{\sin(qR)}{qR} + q^2 \right], \quad (1)$$

where R is determined from

$$\sinh(pR)/pR = \epsilon_1(0, 0). \quad (2)$$

Resta has shown that the results of Eqs. (1) and (2) are in excellent agreement with either the Penn-model or random-phase approximation dielectric functions.¹² For polyacetylene we use $k_f = 1.068$ a.u. and $\epsilon_1(0, 0) = 10$. The resulting $\epsilon_1(q, 0)$ is, of course, only an approximation and does not account for the anisotropy of the dielectric response in polyacetylene.

The measured energy-loss spectra are proportional to $\text{Im}[-1/\epsilon(q, E)]$, and the constant of proportionality is readily determined from $\epsilon_1(q, 0)$ by the requirement

$$\text{Re} \left[\frac{1}{\epsilon(q, 0)} \right] = 1 + \left[\frac{2}{\pi} \right] \int_0^\infty \text{Im} \left[\frac{-1}{\epsilon(q, E)} \right] \frac{dE}{E}. \quad (3)$$

The real and imaginary parts of the dielectric function, $\epsilon_1(q, E)$ and $\epsilon_2(q, E)$, then follow from a standard Kramers-Kronig analysis.^{13,14} Since multiple inelastic scattering was relatively insignificant in these samples, no corrections for it were made in the final analysis. As a test of this approximation, several methods were used to remove the

multiple-scattering events, but they had very little effect on the resulting momentum-dependent dielectric function in the region below 10 eV. The imaginary part of ϵ is presented in Fig. 2. The $q=0.1 \text{ \AA}^{-1}$ spectrum is in good qualitative agreement with the analysis of earlier data¹⁰ although the precise location of the very strong peak at the fundamental edge is about 0.3 eV lower in the present calculation. The main information which we hope to glean from Fig. 2 involves a qualitative understanding of how the spectrum changes with momentum and does not depend on the absolute magnitude of the dielectric function. Moreover, the relative positions of structure in $\epsilon_2(q, E)$ will be more important than their absolute location.

In Fig. 2 the imaginary part of the dielectric response shows a very strong peak at 1.5 eV for $q=0.1 \text{ \AA}^{-1}$ followed by a continuum of excitations extending to higher energy. The shape of this spectrum is in good agreement with $\epsilon_2(0, E)$ computed for a tight-binding band-structure model of $(\text{CH})_x$ in which matrix elements are explicitly calculated.¹⁵ Below ~ 7 eV the excitations are all associated with the π bands of polyacetylene. At 8.7 eV is a rather dispersionless peak associated with the more tightly bound σ electrons. This feature is similar to backbone excitations in polyethylene, as might be expected.¹⁶ As momentum increases, the spectrum of π -electron excitations evolves into two features, a higher-energy peak which broadens increasingly with momentum and shifts to 4.8 eV at 0.7 \AA^{-1} , and a lower-energy peak which is sharper and which appears at 2.4 eV

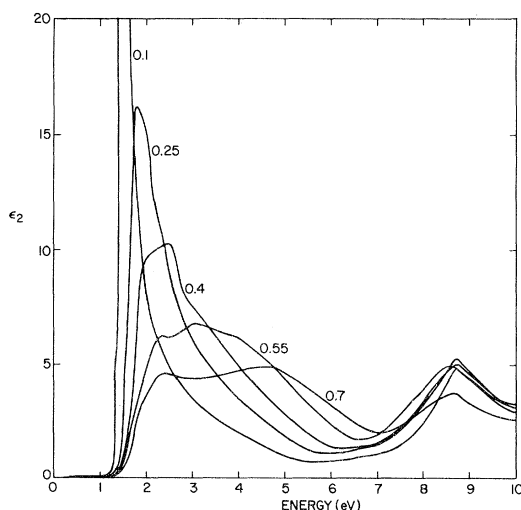


FIG. 2. Imaginary part of the dielectric function of polyacetylene as a function of momentum q in \AA^{-1} .

at $q=0.7 \text{ \AA}^{-1}$. The overall strength in the spectrum shifts to higher energy with increasing q and this is responsible for the positive dispersion of the plasmon shown in Fig. 1(a). Moreover, the magnitude of ϵ_2 in the region from 4 to 7 eV increases with increasing q , thus damping the plasmon at higher momentum.

The broad high-energy peak which appears at 4.8 eV at 0.7 \AA^{-1} can only be associated with single-particle interband transitions in the broad π bands. Insight into the expected momentum dependence of interband transitions in polyacetylene can be gained from the following simple tight-binding model of the π bands. Consider a linear chain of carbon atoms whose p_z orbitals interact with nearest-neighbor transfer integrals β_1 , β_2 , corresponding to alternating double- and single-bond lengths along the chain. In this model the energy bands for $k_{||}$ along the chain are

$$E_{||}(k) = \pm(\beta_1^2 + \beta_2^2 + 2\beta_1\beta_2\cos k_{||}a_{||})^{1/2}, \quad (4)$$

where $k_{||}$ is the electron momentum, $a_{||}$ is the unit-cell length, and the zero of energy is taken at the Fermi energy which is in the center of the gap between the valence and conduction bands. These bands are sketched in the inset to Fig. 3. The gap between valence and conduction bands, E_G , is $2|\beta_1 - \beta_2|$ and the energy of the bandwidth (BW) between the bottom of the valence band and the top of the conduction band is $2(\beta_1 + \beta_2)$. This model can provide a good fit to the results of more

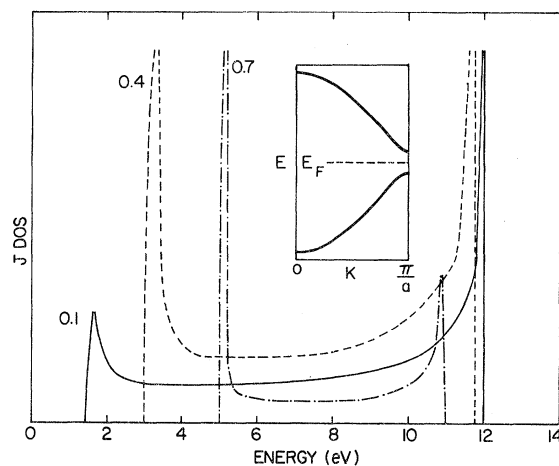


FIG. 3. Joint density of states as a function of momentum in \AA^{-1} for interband excitations for the band structure shown in the inset. Data for different momenta are not normalized relative to each other.

exact calculations.³ Typical values for the transfer integrals obtained from such a fit are 3.35 and 2.65 eV yielding $\Delta=1.4$ eV and BW equals 12 eV.

The calculation of the energy-loss probability or the dielectric function involves the calculation of all possible interband transitions weighted by the matrix elements for each transition. Since these calculations are rather difficult we will neglect the matrix elements and approximate $\epsilon_2(q, E)$ by the joint density of states as a function of momentum for transitions between the bands given in Eq. (4). The one-dimensional joint density of states $J(q, E)$ is given by

$$J(q, E) = (1/2\pi) \int \delta(E - E_c(k_{\parallel} + q_{\parallel}) + E_v(k_{\parallel})) dk_{\parallel}, \quad (5)$$

where E_c is the conduction-band energy, E_v the valence-band energy, and the sum over the Brillouin zone shown in the inset to Fig. 3 is taken for both $\pm q$. With the use of the transfer integrals given above, the spectra are sketched in Fig. 3. The spectrum of direct interband transitions shows a peak at the leading edge which, at small q , is due to the singularities at the valence and conduction edges at the zone boundary. This feature shows strong positive dispersion with increasing q . Above the q -dependent absorption edge is a continuum extending to higher energies.

It is straightforward to extend these calculations to a two-dimensional energy band structure which may be a reasonable approximation for $(\text{CH})_x$ (Ref. 3). The bands perpendicular to the chain direction are relatively narrow (~ 0.3 eV) (Ref. 3) and can be approximated by the tight-binding relation

$$E_{\perp} = \pm (W/2)(1 - \cos k_{\perp} a_{\perp}), \quad (6)$$

where W is the bandwidth of individual conduction and valence bands which are the positive and negative bands, respectively. The unit-cell length perpendicular to the chain direction a_{\perp} is 4.24 \AA ,¹⁷ while a_{\parallel} is 2.44 \AA . The form of Eq. (6) was assumed so as to make a semiconductor with a direct gap at the zone boundary along the chain direction.³ The joint density of states in Eq. (5) is now calculated over the two-dimensional Brillouin zone. In addition, at a given magnitude of the momentum transfer we average over all directions of the momentum vector in the planar Brillouin zone. The resulting joint density of states at $q=0.1$ and 0.7 \AA^{-1} is shown in Fig. 4. It is interesting to note the difference between these curves and the one-dimensional results given in Fig. 3. One effect of averaging over the directions of the momentum

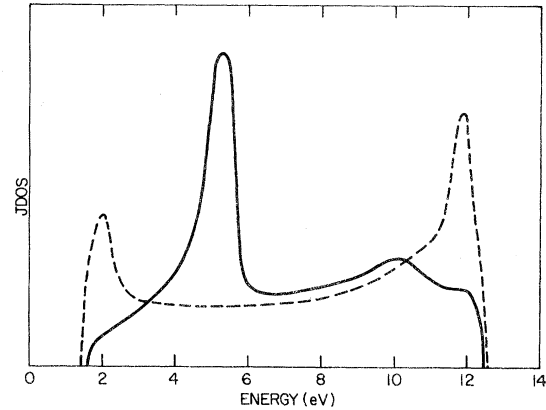


FIG. 4. Joint density of states at $q=0.1 \text{ \AA}^{-1}$, dashed curve, and $q=0.7 \text{ \AA}^{-1}$, solid curve, for interband excitations in a two-dimensional band-structure model taking account of random crystal orientation.

transfer and including excitations transverse to the chain is to broaden the singularities considerably, although they do not shift significantly in energy. In addition, an absorption spectrum extending virtually from the band gap to the maximum allowable transitions will be expected at all values of the momentum transfer. Nevertheless, the strongest feature in the spectrum coincides with that derived from the simpler one-dimensional calculation, and we will use these simpler results in the discussion which follows.

The spectra in Fig. 3 show a very strong peak in the region 10–12 eV due to the flatness of the energy bands at the zone center. While this peak does appear in the joint density of states, it is not observed in $\epsilon_2(q, E)$ since the zone-center transitions are forbidden.^{5,15,18} An easy way to see this is to consider polyacetylene first as a chain with equal bond lengths. Then the π electrons would form a half-filled metallic band in double the Brillouin zone of Fig. 3. This structure is shown as the inset to Fig. 5. Since one-dimensional metals are unstable, the Peierls distortion produces a slight bond-length alternation which introduces a gap at the Fermi level, but does not alter states at $k=0$ or $2\pi/a$. Folding the Brillouin zone of Fig. 5 at π/a results in the band structure of Fig. 3. However, since excitations between $k=0$ and $k=2\pi/a$ are not allowed for the structure in Fig. 5 they will also be forbidden for the bands of Fig. 3.

From the above considerations it may be more illustrative of actual interband transitions in polyacetylene if we approximate them by the joint density of states calculated for the bands in the inset to Fig. 5. This results in the very narrow peaks

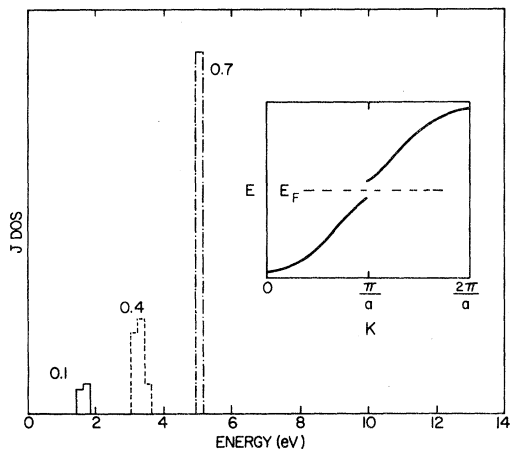


FIG. 5. Joint density of states as a function of momentum in \AA^{-1} for interband excitations for the band structure shown in the inset.

shown in Fig. 5. The strength of the peaks in the joint density of states increases with increasing q because a greater number of states in k space show allowed interband transitions at large q . The distribution is very narrow for q between 0.5 and 0.8 \AA^{-1} because the energy bands have a large region in k space which is nearly linear and parallel. The near linearity of valence and conduction bands over a large region of momentum space means that the peak in the spectrum of interband transitions shows nearly linear dispersion. This relation is given in Fig. 6 where the points with "error bars" give the peak and the width of the interband density of states for the bands in Fig. 5. Also shown in Fig. 6 is the previously published plasmon dispersion.⁸ The unusual linear dependence of the plasmon dispersion seems understandable when correlated with the interband spectra in Fig. 6. Both curves are linear with comparable slopes. The slope of the plasmon dispersion is somewhat less than that of the interband spectra. The main reason for this is that the strength of the plasma oscillation becomes weaker at larger q , eventually leading to a spectrum which is dominated by single-particle excitations.¹⁹ At sufficiently large q the plasmon dispersion becomes tangent to the single-particle spectrum for one-dimensional materials.²⁰ Therefore, the linear dispersion of the plasmon in polyacetylene is largely a consequence of the broad tight-binding energy bands and the fact that (apart from small regions of momentum space at $k = \pi/a$ and the zone boundaries) the valence and conduction bands are nearly linear and

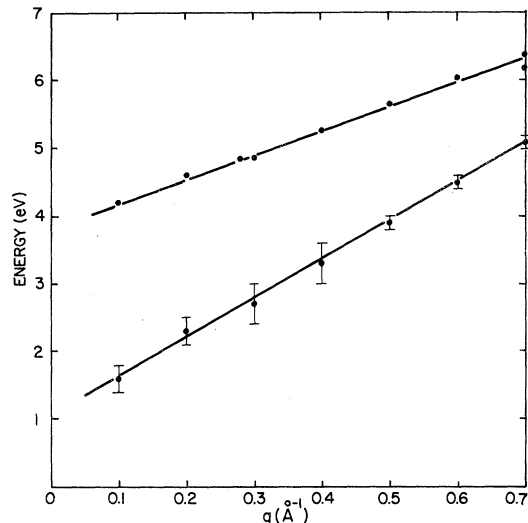


FIG. 6. Interband spectra and plasmon dispersion: Solid dots with "error bars" are center and width of interband spectra using the band structure in Fig. 5; plain dots are plasmon energies from Ref. 8.

parallel over much of the zone. A similar behavior should be expected in other one-dimensional systems, such as polydiacetylene and perhaps other organic polymers with an extended π -electronic structure.

It is interesting to carry the calculation to much larger values of momentum for interband transitions in the band-structure model of Fig. 5. The resulting one-electron excitation spectrum for a one-dimensional semiconductor with a small Peierls gap is shown as the shaded area in Fig. 7, where values of the band width and energy gap appropriate to *trans*-polyacetylene are used. The important parameter is the scale of the momentum q . The excitation spectrum extends to $2\pi/a = 2.6 \text{\AA}^{-1}$ which is very much larger than the region measured in the present work. The measured plasmon dispersion is shown as the solid line. Extrapolating this line, we expect the plasmon to intersect or become tangent to the single-particle spectrum above $q = 1 \text{\AA}^{-1}$. Beyond this value the excitation spectrum will be dominated by single-particle excitations which broaden rapidly with increasing momentum.

The present results provide an interesting contrast to one-dimensional plasmon dispersion in tetrathiafulvalene-tetracyanoquinodimethane (TTF-TCNQ) in which the excitations are also those of a one-dimensional tight-binding electron gas.^{20,21} In TTF-TCNQ the small- q plasmon energy exceeds the bandwidth. As momentum in-

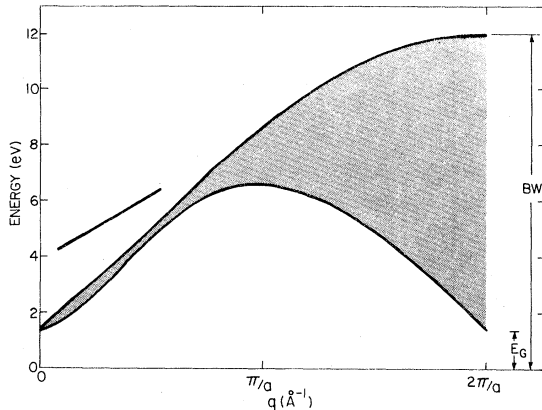


FIG. 7. Shaded area shows the single-particle interband spectrum of polyacetylene with energy gap $E_G = 1.4$ eV, and bandwidth BW equals 12 eV. The solid line is the measured plasmon energy.

creases the plasmon approaches the single-particle continuum and necessarily exhibits negative dispersion.²¹ In the present case the bandwidth is much larger than the small- q plasmon energy, and the plasmon is driven to higher energy with increasing momentum. In addition, in TTF-TCNQ the Brillouin zone is much smaller than in $(\text{CH})_x$ since the length between overlapping π electrons is much longer. Thus, in TTF-TCNQ the plasmon dispersion could be measured across the whole Brillouin zone and, from measurements at the zone boundary, the one-electron bandwidth was determined.²¹ Hence, if the present experimental measurements could be extended to $q \sim 2.6 \text{ \AA}^{-1}$, the spectrum would provide a measure of the π -electron bandwidth of *trans*-polyacetylene as anticipated.⁸ Owing to low scattering probabilities and the problems of radiation damage at long exposure times, these experiments are not feasible at this time.

In addition to the broad high-energy peak at 4.8 eV at $q = 0.7 \text{ \AA}^{-1}$ there is a narrower low-energy peak in ϵ_2 at 2.4 eV which cannot be easily associated with interband excitations with momentum transfer parallel to the chains. In fact, this feature is not expected even when excitations transverse to the chain are included, as shown in Fig. 4. At large q there is much more strength in the region between 2 and 3 eV than would be expected from the joint density of states alone, as can be seen by comparing Figs. 2 and 4. The inclusion of one-electron interband transition matrix elements will affect the distribution of oscillator strength, but it is unlikely that they would enhance the low-energy region at the expense of the higher-energy peak near 5 eV for $q = 0.7 \text{ \AA}^{-1}$. At large momenta the

selection rules are such that all excitations are allowed. Hence, the dielectric function can be reasonably approximated by the joint density of states in the absence of excitonic effects.

The most likely explanation for the peak at 2.4 eV in the large- q spectra is that it indicates an excitonic enhancement of the absorption edge if it is not itself a dispersed exciton. An exciton at the fundamental absorption edge of polyacetylene is not unreasonable. In polydiacetylenes which have a very similar π -electronic structure, there is a good deal of evidence that the fundamental absorption edge is an exciton with a binding energy of about 0.5 eV.²² The very strong peak in ϵ_2 at the absorption onset at low momenta ($< 0.1 \text{ \AA}^{-1}$) is much stronger than would be expected on the basis of the joint density of states alone when the two-dimensional band-structure model is used as seen in Fig. 4. This suggests either very strong matrix element effects or excitonic enhancement of the edge. Furthermore, the lack of a distinct onset attributable to direct interband transitions above the initial exciton is not evidence that the edge is not excitonic. The oscillator strength of an excitonic series joins smoothly to the continuum,²³ and if spectral broadening is sufficient, the direct interband transition onset may not be detectable.

One difficulty with the interpretation of the low-energy peak as a dispersed exciton is that since exciton dispersion relations have not been calculated for this system it is not possible to decide whether or not the observed exciton dispersion is reasonable. For simple spherical electron and hole bands the dispersion relation is²³

$$E = \hbar^2 q^2 / [2(m_e + m_h)], \quad (7)$$

where m_e, m_h are the electron and hole masses, respectively. This model has been applied to exciton dispersion at the fundamental edge of LiF.²⁴ For momenta along the chain direction the energy bands of Eq. (4) yield an effective electron and hole mass at $k = \pi/a$ of ~ 0.1 electron masses. Using Eq. (7) this simple model predicts that the exciton will disperse from 1.5 to 4.7 eV at 0.4 \AA^{-1} , far in excess of the measured low-energy peak. However, a more precise calculation may be able to restore agreement with the measured spectrum since the energy bands in polyacetylene are far from isotropic. Moreover, when q is increased the effective mass of valence- and conduction-band states, out of which the exciton is formed, quickly increases. Both of these effects will tend to decrease the dispersion.

Thus, although the exact nature of the excitonic

enhancement of the fundamental absorption edge in polyacetylene is not known, our data strongly suggest that such effects are important. More theoretical work on excitons and their dispersion in polymers is called for.

In this paper the imaginary part of the momentum-dependent dielectric function of *trans*-polyacetylene was calculated from electron-energy-loss measurements. The only assumption which went into this calculation was the form of $\epsilon(q,0)$, and the qualitative results are relatively insensitive to this quantity. A very strong peak in ϵ_2 at the fundamental absorption edge at small momentum was shown to evolve into two features at large q . The first is a weakly dispersing low-energy peak which we have interpreted as excitonic enhancement of the single-particle spectrum. The low-energy region of the spectrum appears to be enhanced relative to calculated single-particle spectra at all values of the momentum transfer. The

second higher-energy feature in ϵ_2 shows much stronger dispersion and appears to agree reasonably well with the spectrum of direct interband transitions in the broad π bands as computed with simple models. These tight-binding model calculations of interband transitions indicate nearly linear dispersion for the strong features in the interband spectra over the region of momentum space measured. This correlates well with the observed plasmon dispersion. Hence, linear plasmon dispersion can be expected in a wide variety of organic semiconductors characterized by broad quasi-one-dimensional energy bands with relatively narrow gaps.

I am grateful to E. J. Mele for many informative discussions and to A. J. Heeger and the multidisciplinary group at the University of Pennsylvania who supplied the samples.

-
- ¹J. L. Bredas, R. R. Chance, R. Silbey, G. Nicolas, and P. Durand, *J. Chem. Phys.* **75**, 255 (1981), and references therein.
- ²C. B. Duke, A. Paton, W. R. Salaneck, H. R. Thomas, E. W. Plummer, A. J. Heeger, and A. G. MacDiarmid, *Chem. Phys. Lett.* **59**, 146 (1978).
- ³P. M. Grant and I. P. Batra, *Solid State Commun.* **29**, 255 (1979).
- ⁴I. I. Ukrainskii, *Phys. Status Solidi B* **106**, 55 (1981), and references therein.
- ⁵N. A. Cade, *Chem. Phys. Lett.* **53**, 45 (1978).
- ⁶M. Kertesz, *Chem. Phys.* **44**, 349 (1979).
- ⁷C. R. Fincher, M. Ozaki, M. Tanaka, D. Peebles, L. Lauchlan, A. J. Heeger, and A. G. MacDiarmid, *Phys. Rev. B* **20**, 1589 (1979).
- ⁸J. J. Ritsko, E. J. Mele, A. J. Heeger, A. G. MacDiarmid, and M. Ozaki, *Phys. Rev. Lett.* **44**, 1351 (1980).
- ⁹N. C. Banik, *Phys. Rev. B* **24**, 3564 (1981).
- ¹⁰J. J. Ritsko, *Mater. Sci.* **7**, 337 (1981).
- ¹¹R. D. Bringans and W. Y. Liang, *J. Phys. C* **14**, 1065 (1981).
- ¹²R. Resta, *Phys. Rev. B* **16**, 2717 (1977).
- ¹³J. J. Ritsko, L. J. Brillson, R. W. Bigelow, and T. J. Fabish, *J. Chem. Phys.* **69**, 3931 (1978).
- ¹⁴J. J. Ritsko and R. W. Bigelow, *J. Chem. Phys.* **69**, 4162 (1978).
- ¹⁵W. P. Su, J. R. Schrieffer, and A. J. Heeger, *Phys. Rev. B* **22**, 2099 (1980).
- ¹⁶J. J. Ritsko, *J. Chem. Phys.* **70**, 5343 (1979).
- ¹⁷C. R. Fincher, Jr., C. E. Chen, A. J. Heeger, and A. G. MacDiarmid, *Phys. Rev. Lett.* **48**, 100 (1982).
- ¹⁸H. J. Schulz, *Phys. Rev. B* **18**, 5756 (1978).
- ¹⁹D. Pines, *Elementary Excitations in Solids* (Benjamin, New York, 1964).
- ²⁰P. F. Williams and A. N. Bloch, *Phys. Rev. B* **10**, 1097 (1974).
- ²¹J. J. Ritsko, D. J. Sandman, A. J. Epstein, P. C. Gibbons, S. E. Schnatterly, and J. R. Fields, *Phys. Rev. Lett.* **34**, 1330 (1975).
- ²²L. Sebastian and G. Weiser, *Phys. Rev. Lett.* **46**, 1156 (1981).
- ²³R. J. Elliott, *Phys. Rev.* **108**, 1384 (1957).
- ²⁴S. E. Schnatterly, *Solid State Physics*, edited by F. Seitz and D. Turnbull (Academic, New York, 1979), Vol. 34, p. 275.

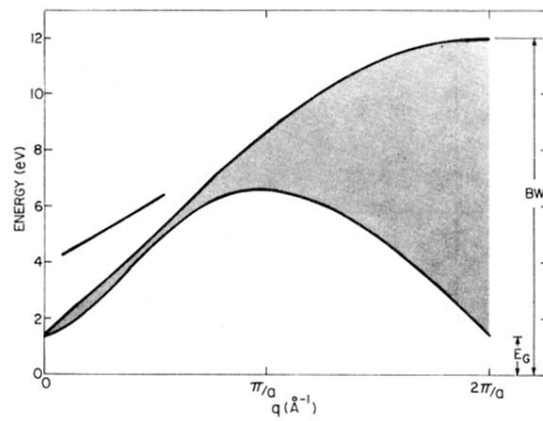


FIG. 7. Shaded area shows the single-particle inter-band spectrum of polyacetylene with energy gap $E_G=1.4$ eV, and bandwidth BW equals 12 eV. The solid line is the measured plasmon energy.